nature photonics

LETTERS

PUBLISHED ONLINE: 23 MAY 2010 | DOI: 10.1038/NPHOTON.2010.117

Mid-infrared wavelength conversion in silicon waveguides using ultracompact telecom-band-derived pump source

Sanja Zlatanovic[1]*†, Jung S. Park[1]†, Slaven Moro[1], Jose M. Chavez Boggio[1], Ivan B. Divliansky[2], Nikola Alic[1], Shayan Mookherjea[1] and Stojan Radic[1]

Mid-infrared light sources are essential for applications that include free-space communication, chemical and biomolecular sensing and infrared spectroscopy[1-3], but no devices comparable to those in the near-infrared regime have emerged to date. Indeed, sources operating above 1.8 μm, including optical parametric oscillators and thulium-doped fibre lasers, do not combine a large tunable range and narrow linewidth, and generally cannot be modulated to support advanced applications[4,5]. Widely tunable mid-infrared quantum cascade lasers are available; however, room-temperature operation in the 3–4 μm range still presents a challenge because of material limitations[6,7]. Wavelength conversion in silicon offers promise for the development of an ultracompact mid-infrared source that combines wide wavelength tuning, narrow linewidth and arbitrarily complex modulation rivalling those in the telecom window. Here, we report four-wave mixing in silicon waveguides in the spectral region beyond 2 μm, using probe and pump waves derived from ultracompact telecom fibre-optic sources, achieving generation of 2,388 nm light.

Considerable effort has been made recently towards achieving spectrally distant parametric wavelength conversion and amplification on a silicon chip[8]. The spectral region beyond 2 μm is of interest for silicon four-wave mixing (FWM), because two-photon absorption (TPA) and the resulting free-carrier absorption (FCA) are reduced as the combined energy of two photons becomes less than the bandgap energy of silicon[3,9]. Thus, silicon could potentially be an attractive parametric nonlinear optics platform for applications in which a mid-infrared (MidIR) source is of vital importance. Recently, four-wave mixing near the 2.2-μm TPA threshold wavelength has been demonstrated with picosecond pump pulses generated from a Ti:sapphire laser and an optical parametric oscillator (OPO) with peak pump power exceeding 20 W, coupled into a large-area (700 nm × 425 nm) silicon waveguide[10]. Unfortunately, conventional OPO pumping is not compatible with the ultimate goal of compact, low-power and modulation-capable parametric devices. More importantly, the picosecond-long pulses do not make use of the advantage of reduced TPA and FCA at 2 μm, and provide limited functionality in free-space communication

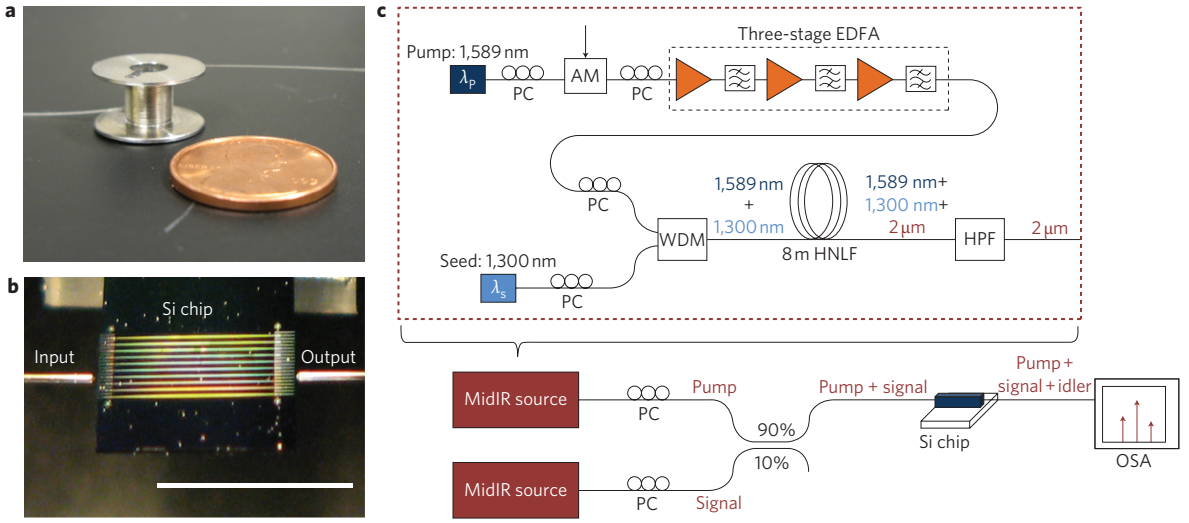

Figure 1 | Measurement set-up. a, Size of the fibre-based MidIR source. **b**, Silicon chip coupled to input and output fibres. Scale bar, ~4 mm. **c**, Schematic of the measurement set-up, including the fibre-optic MidIR source. PC, polarization controller; EDFA, erbium-doped fibre amplifier; AM, amplitude modulator; WDM, wavelength division multiplexer; HPF, high-pass filter; OSA, optical spectrum analyzer.

[1]Department of Electrical and Computer Engineering, University of California San Diego, 9500 Gilman Drive, La Jolla, California 92093, USA, [2]CREOL, The College of Optics and Photonics, University of Central Florida, PO Box 162700, Orlando, Florida 32816-2700, USA; †These authors contributed equally to this work. *e-mail: szlatanovic@ucsd.edu

and sensing applications. To address these limitations, we have designed and demonstrated a MidIR silicon waveguide mixer driven by compact and telecom-compatible sources.

We report a demonstration of a low-power MidIR silicon mixer and demonstrate generation of light up to 2,388 nm using a pump generated by a quasi-continuous-wave (c.w.) fibre light source. FWM was performed with long pump pulses, the duration (1 ns) of which was comparable with the free carrier lifetime in silicon. We have measured a nonlinear parameter γ of 97.3 $(W\ m)^{-1}$at 2.025 μm, which is in agreement with results recently reported at TPA threshold wavelengths[10]. These results clearly demonstrate the viability of silicon as a MidIR nonlinear platform that is inherently compatible with telecom pumping technology. The fibre-based MidIR source can be spooled to a millimetre-scale radius, as illustrated in Fig. 1a, allowing the elements of the MidIR source architecture to have comparable size scales (Fig. 1b). Combined with standard pumping diodes, this source retains an ultracompact footprint and provides bandwidth and tuning over a spectral range not achievable with silicon MidIR Raman-based devices[2,11].

The fibre-optic 2-μm pump and probe waves were generated by the degenerate parametric process between a 1,300-nm seed diode laser and standard (telecom-band) pump at 1,589 nm in a highly nonlinear fibre (HNLF)[12,13], as shown in Fig. 1c. A tunable c.w. laser at 1,589 nm was amplitude-modulated to produce 1-ns pulses at a repetition rate of 1 MHz, then amplified and combined with a tunable seed near 1,300 nm. Mixing in the 8-m-long HNLF section generated an idler in the 2-μm band with 1 W of peak power. Two independent HNLF mixers were constructed to generate the tunable probe and the pump in the 2-μm band. The first mixer was seeded by a 1,307.5-nm fixed diode laser to produce a 2,025-nm pump, and the second was seeded by a diode laser tunable between 1,260 and 1,360 nm to generate a tunable probe between 1,912 and 2,155 nm. After high-pass filtering to reject the near-infrared (NIR) components, the generated 2-μm pump and probe waves were combined with a 90/10 coupler then inserted into the silicon chip using a lens-tipped fibre. The silicon mixer output was fibre-coupled and observed in an extended-range optical spectrum analyser capable of measuring wavelengths up to 2.4 μm.

The silicon waveguides were fabricated from silicon-on-insulator (SOI) wafers (15 Ω cm) using standard electron-beam lithography and dry etching techniques. The waveguides had cross-sectional areas of 1,060 nm (width) × 250 nm (height) and lengths of 3.8 mm, not including the polymer-overcoated inverse tapers for coupling to input and output lens-tipped fibres, as illustrated in Fig. 1b. The total input/output fibre-to-fibre loss at 2,025 nm was 15 dB. In contrast to the work reported in ref. 10, these waveguides were formed from the same wafers and had the same device height as the SOI wafers used at telecom (1,550 nm) wavelengths, consistent with the original motivation for this work.

Figure 2a shows the FWM spectra with the pump centred at 2,025 nm while the probe was tuned from 1,912 to 1,994 nm, limited only by the short-wave 1,360-nm tunable seed source. The measured conversion efficiency, plotted in Fig. 2b as a function of pump–probe wavelength detuning, had a peak value of −22.2 dB and was 2 dB equalized across the entire measured range of 241 nm. By assuming reciprocal and equal input and output coupling efficiencies, the peak pump power inside the waveguide was calculated to be only 176 mW, well within the compatibility range of standard telecom-band pump diodes. Theoretical predictions of conversion efficiency computed for the waveguide dimensions, pump wavelength and power used in our experiments (Fig. 2c) show an expected conversion bandwidth of 292 nm.

Measuring the dependence of the conversion efficiency on pump power yielded a value for the silicon mixer nonlinear parameter γ of 97.3 $(W\ m)^{-1}$. Remarkably, taking into account the waveguide

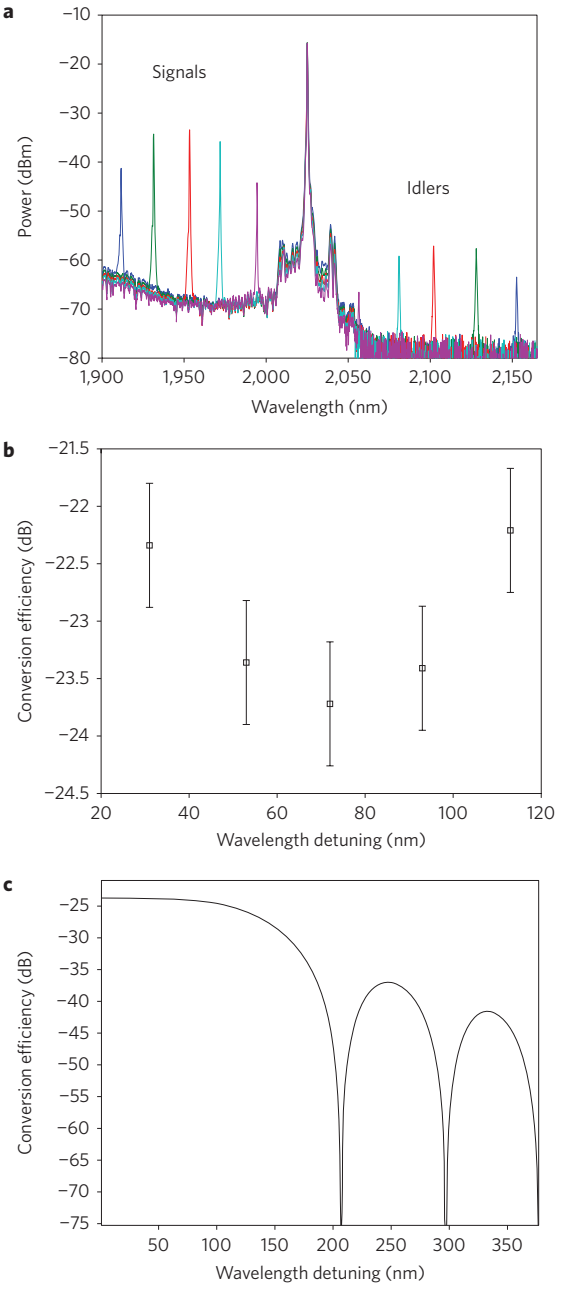

Figure 2 | Four-wave mixing. a, Measured four-wave mixing spectrum across a range of 241 nm. **b**, Measured conversion efficiency versus pump-signal wavelength detuning, illustrating 2-dB equalized conversion over the 241-nm range. The error bars are calculated based on pump power variation during the experiment, which was 0.54 dB. **c**, Calculated four-wave mixing conversion efficiency for the waveguide parameters and power used in the experiment, showing that the predicted conversion bandwidth of 292 nm is in good agreement with measurements.

modal area $A_{\mathrm{eff}} = 0.348\ \mu m^2$ computed using finite element method, the nonlinear parameter $n_2 = 10.8 \times 10^{-18}\ m^2\ W^{-1}$ is highly consistent with previously reported measurements of the silicon Kerr coefficient[11]. More importantly, this measurement, when combined with the reported 2-μm TPA coefficient β_{TPA} in bulk silicon[14,15], defines a tenfold increase in the 2-μm-band nonlinear figure of merit (FOM), $n_2/(\lambda\beta_{\mathrm{TPA}})$, over that of the standard telecom (1,550 nm), demonstrating the true potential of silicon as a platform for parametric nonlinear optics outside the NIR band. Although silicon nonlinearity is expected to decrease at longer

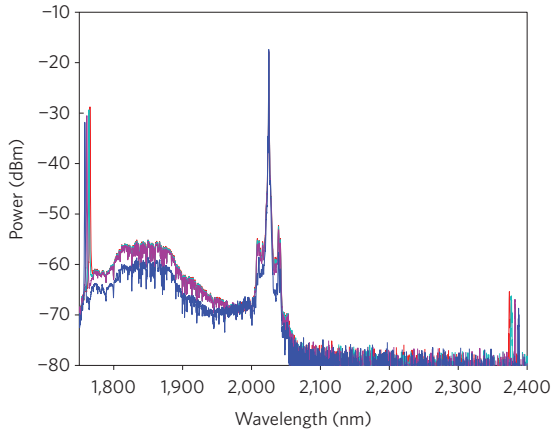

Figure 3 | Four-wave mixing spectra. Spectra illustrating up to 630-nm-wide conversion, showing the idler generated at 2,388 nm with a conversion efficiency of −36.8 dB. Idler power is corrected for output fibre loss measured at the idler wavelength.

wavelengths, there is a reasonable expectation that superior FOM values would be maintained in the practically useful spectral range above 2 μm and towards 2.2 μm and beyond[14,15]. No measurable pump impairment due to TPA was observed at all the power levels used in this experiment. Further work on increasing the power of the 2-μm pump source is thus expected to improve the conversion efficiency while retaining the equalized mixer response.

The maximum parametric conversion bandwidth was measured by generating a probe at 1,758 nm with a 1,450-nm seed in the HNLF mixer, and subsequent mixing with the 2,025-nm pump in the silicon waveguide to produce an idler at 2,388 nm, as shown in Fig. 3. Accounting for the measured loss in the output silica fibre at this idler wavelength, an efficiency of −36.8 dB was measured for the 630-nm conversion process. To the best of our knowledge, this is the longest infrared wavelength generated by a first-order FWM conversion process in a silicon chip[16]. Note that the HNLF used in the present experiments could be spooled to a millimetre-scale radius with negligible bend loss for wavelengths up to 2.3 μm (Fig. 1a), showing tremendous promise for an ultra-compact pump source that could be used in conjunction with chip-scale silicon MidIR devices. This work suggests that the HNLF fibre source can easily reach the 2-μm band and parametric conversion in the silicon chip beyond 2.3 μm, at which point the loss of standard silica fibre inhibits efficient light generation. A two-stage mixer driven by a continuously tunable seed in the standard NIR telecom band can therefore be constructed to cover the MidIR spectral range. In contrast to previous attempts to generate 2-μm light in silicon waveguides[16] using a pump near 1,550 nm, this approach is not limited by the nonlinear absorption of the pump, and is thus scalable by engineering the silicon waveguides and infrared source.

In conclusion, we have demonstrated mid-infrared four-wave mixing in silicon waveguides, with a 2-μm pump, generated from a telecom-compatible fibre-optic source. The measurements indicate that the nonlinear parameter γ is comparable to that for the 1,550-nm band and, combined with a reduction in the TPA-induced nonlinear absorption, results in a tenfold improvement of the nonlinear FOM. Consequently, two-stage mixer technology that combines NIR (silica) and MidIR (silicon) waveguides holds considerable potential for application in a wide range of mid-infrared nonlinear optic devices.

Methods

Waveguide fabrication. The silicon waveguides were fabricated from SOI wafers with a 250-nm-thick silicon device layer lying on top of a 3-μm buried oxide (BOX) layer serving as the bottom cladding. The wafers were spin-coated with FOX13 negative-tone electron-beam resist (Dow Corning), patterned by electron-beam lithography, and developed in tetramethylammonium hydroxide (TMAH). The resulting resist pattern served as a hard mask for reactive ion etching (RIE) of the silicon down to the BOX to form the waveguide structure. The 150-μm-long input and output silicon inverse tapers were overlaid with SU-8 polymer waveguides (cross-section, 5 μm × 2 μm; length, 1 mm) by photolithography. The chips were then lapped and cleaved to form the input and output facets, and mounted for testing.

Characterization of waveguide losses. Light was coupled into and out of the waveguides using lens-tipped fibres and spot-size converters. The spot-size converters were composed of SU-8 polymer waveguides overlying the inverse silicon taper as described. The waveguide propagation loss of 2.8 dB cm^{-1} was measured at 1,550 nm using the cutback method. A similar propagation loss is assumed at 2,025 nm, because the scattering loss due to waveguide surface imperfections is lower at longer wavelengths[17] and the intrinsic loss in both the SiO_2 and silicon[18] is in the same range as at 1,550 nm. The total propagation loss of the 3.8-mm-long waveguide was ~1 dB. The measured total insertion loss at 2.025 μm was 15 dB. We confirmed, using two-dimensional simulation, that the input and output spot-size converters had similar coupling losses. Because they were reciprocal and the input and output lensed-tipped fibres had identical numerical apertures, we concluded that the input and output coupling losses were equal. Therefore, subtracting the propagation loss from total loss, we were able to estimate the coupling loss to be 7 dB per coupler at both input and output. The high coupling loss can be attributed to modal mismatch between the lens-tipped fibres and the polymer waveguides, misalignment of the silicon taper and polymer overlay during fabrication, and insufficient taper length.

Effective index calculations. Waveguide effective indices were calculated for the transverse electric (TE) mode using a finite-element method mode solver (COMSOL) in the wavelength range between 1,300 and 3,000 nm. Sellmeier equations were used to incorporate dispersion of silicon and SiO_2. The dispersion of hydrogen silsesquioxane (HSQ), a leftover cross-linked FOX13 resist on top of the silicon, was assumed to be the same as that of SiO_2. The mode profile at the pump wavelength is given in Supplementary Fig. S1.

Measurements of nonlinearity. To quantify γ, we measured the dependence of conversion efficiency on pump power (Supplementary Fig. S2) and extracted the coefficient by fitting the curve with

$$G(P_0) = (\gamma P_0/g)^2 \times \sinh^2(gL) \quad (1)$$

where L is the waveguide length, $g = \sqrt{(\gamma P_0)^2 - ((\Delta k + 2\gamma P_0)/2)^2}$ and $\Delta k = 2\pi((n_s/\lambda_s) + (n_i/\lambda_i) - 2(n_p/\lambda_p))$, and n_s, n_i and n_p are effective indices at signal, idler and pump wavelengths, respectively, obtained from finite-element simulations.

Conversion efficiency was measured from the spectra. The input peak pump power was obtained by adding the output coupler and propagation losses to the average power and 30 dB to account for the 1:1,000 repetition rate. The value of γ obtained was 97.3 (W m)$^{-1}$.

Calculations of conversion efficiency. The conversion efficiency plot in Fig. 2c was calculated using equation (1), with a waveguide length $L = 3.8$ mm, pump power $P_0 = 176$ mW, $\gamma = 97.3$ (W m)$^{-1}$ (obtained experimentally) and Δk, calculated for a range of signal–idler wavelength pairs.

Received 3 November 2009; accepted 24 March 2010; published online 23 May 2010

References

1. Ebrahim-Zadeh, M. & Sorokina, I. T. *Mid-Infrared Coherent Sources and Applications* (Springer, 2008).
2. Raghunathan, V., Borlaug, D., Rice, R. & Jalali, B. Demonstration of a mid-infrared silicon Raman amplifier. *Opt. Express* **15,** 14355–14362 (2007).
3. Soref, R. A., Emelett, S. J. & Buchwald, W. R. Silicon waveguided components for the long-wave infrared. *J. Opt. A* **8,** 840–848 (2006).
4. Kameyama, S. *et al.* Development of 1.6 μm continuous-wave modulation hard-target differential absorption LIDAR system for CO_2 sensing. *Opt. Lett.* **34,** 1513–1515 (2009).
5. Bashkansky, M., Burris, H. R., Funk, E. E., Mahon, R. & Moore, C. I. RF phase-coded random-modulation LIDAR. *Opt. Commun.* **231,** 93–98 (2004).
6. Wysocki, G. *et al.* Widely tunable mode-hop free external cavity quantum cascade lasers for high resolution spectroscopy and chemical sensing. *Appl. Phys. B* **92,** 305–311 (2008).
7. Cathabard, O., Teissier, R., Devenson, J. & Baranov, A. InAs-based distributed feedback quantum cascade lasers. *Electron. Lett.* **45,** 1028–1030 (2009).
8. Foster, M. A. *et al.* Broad-band optical parametric gain on a silicon photonic chip. *Nature* **441,** 960–963(2006).
9. Raghunathan, V., Shori, R., Stafsudd, O. & Jalali, B. Nonlinear absorption in silicon and the prospects of mid-infrared silicon Raman lasers. *J. Phys. Status Solidi A* **203,** R38–R40 (2006).

10. Liu, X., Osgood, R. M., Vlasov, Y. A. & Green, W. M. J. *Broadband Mid-Infrared Parametric Amplification, Net Off-Chip Gain, and Cascaded Four-Wave Mixing in Silicon Photonic Wires*, 6th International Conference on Group IV Photonics (IEEE, San Francisco, 2009).
11. Rong, H. *et al.* Monolithic integrated Raman silicon laser. *Opt. Express* **14,** 6705–6712 (2006).
12. Boggio, J. M. C. *et al.* Tunable parametric all-fiber short-wavelength-IR transmitter. *J. Lightwave Technol.* **28,** 443–447 (2010).
13. Boggio, J. M. C. *et al.* Short wavelength infrared frequency conversion in ultra-compact fiber device. *Opt. Exp.* **18,** 439–435 (2010).
14. Bristow, A. D., Rotenberg, N. & van Driel, H. M. Two-photon absorption and Kerr coefficients of silicon for 850–2,200 nm. *Appl. Phys. Lett.* **90,** 191104 (2007).
15. Lin, Q. *et al.* Dispersion of silicon nonlinearities in the near infrared region. *Appl. Phys. Lett.* **91,** 021111 (2007).
16. Turner-Foster, A. C., Foster, M. A., Salem, R., Gaeta, A. L. & Lipson, M. *Frequency Conversion in Silicon Waveguides Over Two-Thirds of an Octave*, Conference on Lasers and Electrooptics (OSA/IEEE, Baltimore, 2009).
17. Busse, L. E., McCabe, G. H. & Aggarwal, I. D. Wavelength dependence of the scattering loss in fluoride optical fibers. *Opt. Lett.* **15,** 423–424 (1990).
18. Jalali, B. *et al.* Prospects for silicon mid-IR Raman lasers. *IEEE J. Sel. Topics Quantum Electron.* **12,** 1618–1627 (2006).

Acknowledgements

The authors acknowledge the Defense Advanced Research Projects Agency and the National Science Foundation for funding support. J.S.P. acknowledges sponsorship support from the NSF Graduate Research Fellowship Program. The authors thank B.P.P. Kuo, C.S. Brés, E. Myslivets, A. Wiberg and M.L. Cooper for useful discussions and J.E. Ford and E.J. Tremblay for the loan of equipment.

Author contributions

S.Z. assembled the MidIR source, performed the FWM experiments, and carried out data analysis and theoretical computations. J.S.P. designed and fabricated the silicon waveguides, assisted in assembling the MidIR source, performed the FWM experiments and data analysis, and wrote the manuscript. S. Moro and J.M.C.B. assisted with the MidIR source. I.B.D. assisted with the electron-beam lithography process for waveguide fabrication. N.A., S. Mookherjea and S.R. helped plan the project and guided and supervised the experiments. All authors assisted with preparation of the manuscript and discussion of results.

Additional information

The authors declare no competing financial interests. Supplementary information accompanies this paper at www.nature.com/naturephotonics. Reprints and permission information is available online at http://npg.nature.com/reprintsandpermissions/. Correspondence and requests for materials should be addressed to S.Z.